

# Retrieval of critical current distribution in small Josephson junctions

O. Neshera<sup>a)</sup> and E. N. Ribak

Department of Physics, Technion, Technion City, Haifa 32000, Israel

(Received 22 April 1997; accepted for publication 18 June 1997)

We have developed a method to retrieve or to estimate the spatial critical current distribution in a small Josephson junction from a critical current measurement in a magnetic field (the junction size is in reference to the Josephson length). The method is based on an iterative algorithm that uses fast Fourier transform and physical constraints to achieve the proper solution(s). We simulated some typical critical current distributions and the algorithm converged to a single solution. We applied the algorithm to measurements of the critical current of grain boundary junctions of an oxygen deficient  $\text{YBa}_2\text{Cu}_3\text{O}_{7-\delta}$  thin film. The convergence was always to one of a very few solutions very similar in nature. © 1997 American Institute of Physics. [S0003-6951(97)03433-5]

Critical current distribution in a Josephson junction is an important tool for understanding the structure and the magnetic field distribution inside the junction, hence its importance as an analysis tool. For example, uniformity of the critical current in the junction affects noise, as would be manifested in a superconducting quantum interference device (SQUID). Until now the critical current distribution was neither measured nor calculated directly from other measurements. By measuring the critical current of a Josephson junction as a function of the magnetic field  $I_c(B)$ , one can obtain information about the spatial critical current density distribution in the junction  $j_c(x)$ , which will yield information about the real geometry of the junction and about fluxes inside or outside the junction. We first consider a junction of width  $W$  and thickness  $d$ , with a cross section in the  $x$ - $y$  plane and a magnetic field  $B$  applied parallel to the  $y$  direction. A junction is considered small if its width is  $W \ll \lambda_J$ , where  $\lambda_J$  is the Josephson penetration depth  $\lambda_J = \sqrt{\Phi_0/4\pi\mu_0\lambda_L}$ , where  $\Phi_0$  is a unit of magnetic flux ( $2.07 \times 10^{-7}$  G cm<sup>2</sup>) and  $\lambda_L$  is the London penetration depth. In this case we can assume that the magnetic field  $B$  is uniform along the  $x$  direction, and then the phase inside the junction is related to the  $x$  coordinate by

$$\varphi(x) = (2\pi d_m B / \Phi_0)x + \phi_0, \quad (1)$$

where  $d_m = t + 2\lambda_L \cong 2\lambda_L$ . Here,  $t$  is the thickness of the barrier of the junction; usually  $t \ll \lambda_L$ . The critical currents of the junction are related by a Fourier transform:<sup>1</sup>

$$\begin{aligned} I_c(B) &= |J_c(B) e^{i\varphi(B)}| \\ &= \left| \int_0^W j_c(x) e^{i\varphi(x)} dx \right| \\ &= \frac{\Phi_0}{d_m} \left| \mathfrak{J} \left[ j_c \left( \frac{\Phi_0}{d_m} x \right) \right] \right|, \end{aligned} \quad (2)$$

where  $j_c(x)$  is the critical current density and is defined by  $j_c(x) = \int_0^d j_c(x, y) dy$ . Equation (2) contains only partial information on  $j_c(x)$ ; the main problem is the lack of phase of  $\mathfrak{J}[j_c(x)]$ . By performing an inverse Fourier transform on  $|I_c(B)|$  we retrieve the autocorrelation function of  $j_c(x)$ ; this is the most information that we can get directly on

$j_c(x)$ .<sup>2,3</sup> Until now many attempts, mostly by model fitting, were made to reconstruct  $j_c(x)$  from  $I_c(B)$ , i.e., trying to find a model for  $j_c(x)$  whose Fourier amplitudes are most similar to the measured  $I_c(B)$ .<sup>2-6</sup>

We tried to solve this problem by using an algorithm based on the method of projection on convex sets (POCS).<sup>7-9</sup> This algorithm is based on numerical iterative calculation that uses a fast Fourier transform (FFT) and known constraints to recover the lost phase of  $\mathfrak{J}[j_c(x)]$  as follows.

- (1) We start by creating an array of random phases  $\phi_n(B)$  ( $n=0$  initially).
- (2) The phases are added to the measured amplitudes  $I_c(B)$  in the magnetic domain. We get  $I_n(B) = I_c(B) e^{i\phi_n(B)}$ .
- (3) The algorithm then calculates the inverse FFT (IFFT) of  $I_n(B)$  into the real space ( $x$ ) domain, where we get, in general,  $i_n(x) = \mathfrak{J}^{-1}[I_n(B)]$ .
- (4) Here physical constraints are applied to the function  $i_n(x)$  to form a modified current  $i'_n(x)$ . The constraints we choose to use are (a) the critical current must be real,  $i'_n(x) = \text{Re}[i_n(x)]$ ; (b) the critical current must be positive,  $i'_n(x) = i_n(x)$  if  $i_n(x) > 0$ ; (c) the critical current outside the junction should be zero,  $i'_n(x) = 0$  if  $x < 0$  or  $x > W$ ; (d) the current should also be conserved after (a)–(c) are satisfied,<sup>10</sup>  $\sum_x [i'_n(x)] = \sum_x [i_n(x)]$ . This is achieved by multiplying  $i'_n(x)$  by a constant derived from the deleted components.
- (5) We return to the magnetic domain by FFT. We get  $I_{n+1}(B) = \mathfrak{J}[i'_n(x)]$  with a new phase  $\phi_{n+1}(B) = \arg[I_{n+1}(B)]$ .
- (6) We check for convergence. If it is not achieved, we return to step (2); otherwise the solution is  $i_c(x) = i_n(x)$ .

If we get the same solution every time, we start with another set of random phases  $\phi(B)$ ; then we have probably found a single mathematical solution. A unique solution is not guaranteed in such one-dimensional problems.<sup>11</sup>

We tested the algorithm by trying to reconstruct some typical critical current distributions, such as convex or concave distributions,<sup>1</sup> from the amplitudes of their Fourier transforms. For all the symmetric critical current distributions we got, after a few hundred iterations, a convergence to a single solution—the one we started with. When asymmetric critical current distributions were tried, two solutions that

<sup>a)</sup>Electronic mail: oneshera@physics.technion.ac.il

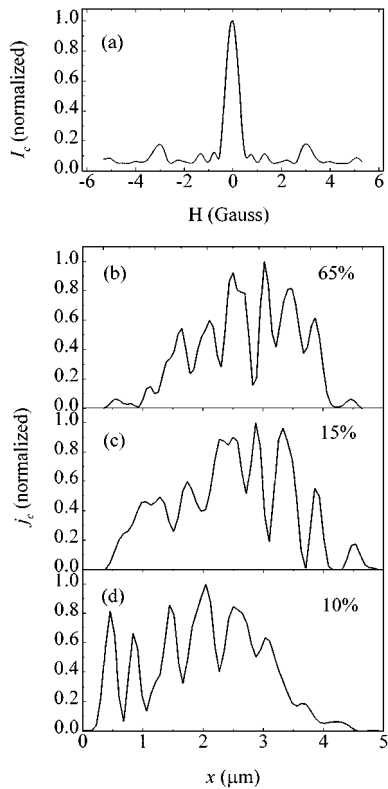


FIG. 1. (a) Critical current of the  $5 \mu\text{m}$  grain boundary junction vs magnetic field; (b)–(d) three of the most common solutions of the critical current distribution and their abundance among all solutions.

were opposite in direction but otherwise equal were found, and one was equal to the original critical current distribution. There is no way to tell the true solution from its mirror image.<sup>11</sup> In order to check sensitivity to noise, we created a uniform critical current distribution with a random Gaussian noise added to it. Multiple solutions start to appear for levels of noise larger than 0.25 of the uniform distribution. This means that, for this level of noise, the starting guess becomes significant.<sup>7</sup>

We tested the method on measurements from a grain boundary junction made of an oxygen deficient  $\text{YBa}_2\text{Cu}_3\text{O}_{7-\delta}$  ( $T_c = 55 \text{ K}$ ) thin film that was deposited by laser ablation on a  $24^\circ$  bicrystal  $\text{SrTiO}_3$  substrate. The film had a  $150 \text{ nm}$  thickness, and its width was patterned to be  $W = 5 \mu\text{m}$ . The critical current of the junction  $J_C(B)$  was measured and the normalized result is shown in Fig. 1(a). The value of the measured critical current without magnetic field was  $32.5 \mu\text{A}$ , and, assuming  $\lambda_L = 170 \text{ nm}$  for  $\text{YBa}_2\text{Cu}_3\text{O}_{7-\delta}$  results in  $\lambda_J = 2.5 \mu\text{m}$ . Under these conditions we may say that to a first approximation the magnetic field in the junction is uniform,<sup>4</sup> and we call this a small junction.

In order to find the critical current distribution we used the phase retrieval algorithm described above. There is a critical current level that is independent of the field, which indicates that  $j_c(x, y)$  contains white noise.<sup>12</sup> There are two ways to deal with such noise. The first is to subtract it from all data, which would mean that we ignore its effect at all magnetic fields, low and high. We have taken a second approach: we only removed the critical current signal at high

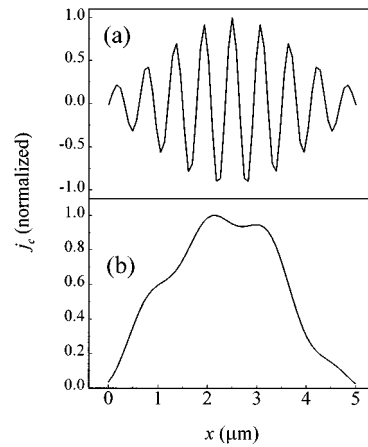


FIG. 2. The two parts of the critical current distribution in the junction: (a) the convex part and (b) the oscillatory part. Their sum is very close to that of Fig. 1(b).

field. This corresponds in the junction domain to removal of noise only at high frequencies. Mathematically, we multiplied it by a tapering filter, a cosine bell function, which drops from unity inside the region ( $|B| < 5 \text{ G}$ ) to zero outside the region ( $|B| > 5 \text{ G}$ ) in the same way that a cosine would change between 0 and  $\pi$ . For our data of 4001 points (after applying the tapering filter) we used a FFT of 8192 points to avoid aliasing.<sup>11</sup> The critical current is slightly asymmetric with respect to the magnetic field because of measurement errors. This is different from our model which assumes a real value for the critical current in the real space ( $x$ ). The results converged to the same junction size: even without using the size constraint, there was no current outside a  $5 \mu\text{m}$  region. When applying a size constraint of  $5 \mu\text{m}$ , convergence was faster, but this constraint was not required *per se*.

After running the algorithm tens of times, each time with initial different random phases, we got six solutions, three of the most common (total 90%) are shown in Fig. 1, with their abundance. All the solutions, although mathematically different, do have the same physical qualities, namely, they share the same size, they all have the same convex distribution, and they only differ by the oscillations on top of this convex distribution. These oscillations share the same frequency, but are superposed at different shifts relative to the convex distribution. The origin of the oscillation is the two bumps at  $\pm 3.1 \text{ G}$  [Fig. 1(a)]. Since these bumps can be easily recognized, we separated the convex part and the oscillations and applied the algorithm to the two parts separately. Now there was no ambiguity and we got only one solution for the convex part and one solution for the oscillatory part (Fig. 2). Adding these two parts gives us a critical current distribution that is similar to the most common solution [Fig. 1(b)].

We tried this algorithm on a larger junction ( $10 \mu\text{m}$ ), where the Fourier relationship is even less valid than for the smaller junction. Unlike the small junction case, where the convergence was to a few solutions, in the case of larger junctions each initial random phase condition led to a different solution (Fig. 3). Again, we can see common features, such as the junction size and a common shape, concave in this case (probably due to the self-field of the current in large

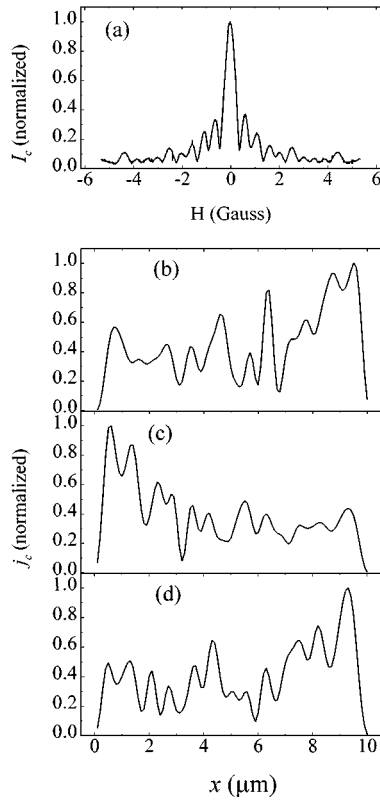


FIG. 3. (a) Critical current of the 10  $\mu\text{m}$  grain boundary junction vs magnetic field, (b)–(d) three typical solutions of the critical current density distribution from the many obtained.

junctions).<sup>1</sup> However, we were not successful in characterizing the oscillations. We were not able to separate them properly from the low frequency (or low magnetic field) current and thus could not solve for the two parts separately.

The origin for the oscillatory part of the current distribution is probably due to the structure of the grain boundary junction. This is because of the strong dependence of the current on the actual barrier thickness  $t$ :<sup>13</sup>

$$j_c(x, y) \propto e^{-\kappa t(x, y)}, \quad (3)$$

where  $\kappa^{-1}$  is the decay length of the barrier. Measurements of the critical current in magnetic field of  $\text{YBa}_2\text{Cu}_3\text{O}_{7-\delta}$  grain boundary junctions were taken by others.<sup>3,4,5,14,15</sup> Hilgenkamp *et al.*<sup>14</sup> noticed the presence of similar peaks in other samples with comparable thicknesses and junction sizes ( $W \sim 16 \mu\text{m}$ ), and attributed these peaks to a semi-regular array of grain boundaries of 0 and  $\pi$  facets at the junction. We measured a sample grown under similar conditions to the 5  $\mu\text{m}$  sample above (Figs. 1 and 2) with an atomic force microscope (AFM) (Fig. 4) and found that the island size was approximately 0.1–0.2  $\mu\text{m}$ , similar to the results quoted.<sup>14,15</sup> Our sample, in contrast to those of Refs. 14 and 15, was grown at in oxygen deficient atmosphere. However, notice that the oscillations (Fig. 2) have a spatial extent of 0.5  $\mu\text{m}$ .

In addition, we calculated the focusing factor of the

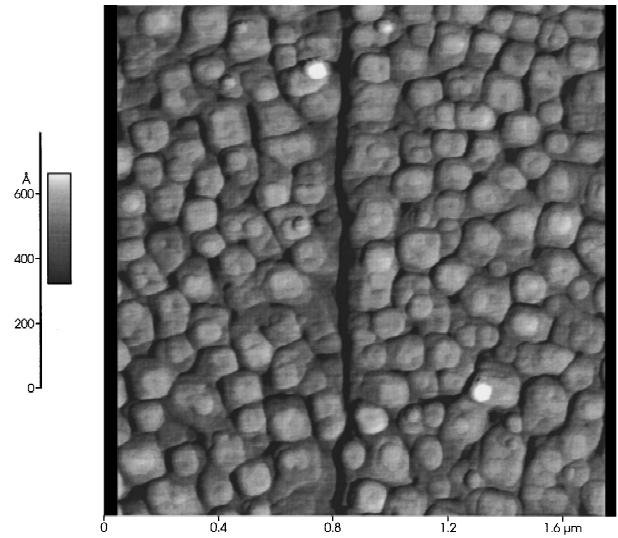


FIG. 4. AFM image of the 150-nm-thick oxygen deficient  $\text{YBa}_2\text{Cu}_3\text{O}_{7-\delta}$  grain boundary on a  $24^\circ$  bicrystal  $\text{SrTiO}_3$  substrate.

magnetic field in the junction. The unit of length in the real domain is  $dx = 1/2k_{\text{max}}$ , where  $k = 2\pi d_m B / \Phi_0$  [Eq. (1)]. The width of the junction is the product of  $dx$  multiplied by the number of length units in the reconstruction and totals 1  $\mu\text{m}$ . The measured width of the junction was 5  $\mu\text{m}$ , which gives a focusing factor of 5.

In summary, we developed a method to retrieve the critical current density distribution in a small Josephson junction, and we tested it against both simulation and real data. We found that for a small, oxygen deficient,  $\text{YBa}_2\text{Cu}_3\text{O}_{7-\delta}$  grain boundary junction the critical current distribution consists of a convex distribution with an oscillation superposed on it.

Acknowledgments are due to P. Richter and R. Gross for making the current measurements, and to G. Koren, E. Polturak, and I. Snapiro for useful discussions.

<sup>1</sup>A. Barone and G. Paterno, *Physics and Application of the Josephson Effect* (Wiley, New York, 1982).

<sup>2</sup>H. H. Zappe, *Phys. Rev. B* **11**, 2535 (1975).

<sup>3</sup>O. M. Froehlich, H. Schulze, A. Beck, R. Gerdemann, B. Mayer, R. Gross, and R. P. Huebener, *IEEE Trans. Appl. Supercond.* **5** (1995).

<sup>4</sup>O. M. Froehlich, H. Schulze, A. Beck, B. Mayer, L. Alff, R. Gross, and R. P. Huebener, *Appl. Phys. Lett.* **66**, 2289 (1995).

<sup>5</sup>P. A. Rosenthal, M. R. Beasley, K. Char, M. S. Colclough, and G. Zaharchuk, *Appl. Phys. Lett.* **59**, 3482 (1991).

<sup>6</sup>S. C. Gausepohi, M. Lee, and K. Char, *Appl. Phys. Lett.* **68**, 2279 (1996).

<sup>7</sup>H. Stark and M. I. Sezan, in *Real-time Optical Information Processing*, edited by B. Javidi and J. L. Horner (Academic, Boston, 1994), Chap. 5.

<sup>8</sup>R. W. Gerchberg and W. O. Saxton, *Optik (Stuttgart)* **33**, 237 (1972).

<sup>9</sup>J. R. Fienup, *Appl. Opt.* **21**, 2578 (1993).

<sup>10</sup>G. R. Ayers and J. C. Dainty, *Opt. Lett.* **13**, 547 (1988).

<sup>11</sup>R. H. T. Bates and M. J. McDonnell, *Image Restoration and Reconstruction* (Clarendon, Oxford, 1986).

<sup>12</sup>I. K. Yanson, *Sov. Phys. JETP* **31**, 800 (1970).

<sup>13</sup>P. G. deGennes, *Rev. Mod. Phys.* **36**, 255 (1964).

<sup>14</sup>H. Hilgenkamp, J. Mannhart, and B. Mayer, *Phys. Rev. B* **53**, 14 586 (1996).

<sup>15</sup>J. Mannhart, H. Hilgenkamp, B. Mayer, Ch. Gerber, J. R. Kirtly, and K. A. Moler, *Phys. Rev. Lett.* **77**, 2782 (1996).